The Pacific sea surface temperature

David H. Douglass

Department of Physics and Astronomy, University of Rochester, Rochester, NY 14627-0171, United States

ABSTRACT

The Pacific sea surface temperature data contains two components: N_L, a signal that exhibits the familiar El Niño/La Niña phenomenon and N_H, a signal of one-year period. Analysis reveals: (1) The existence of an annual solar forcing F_S; (2) N_H is phase locked directly to F_S while N_L is frequently phase locked to the 2nd or 3rd subharmonic of F_S. At least ten distinct subharmonic time segments of N_L since 1870 are found. The beginning or end dates of these segments have a near one-to-one correspondence with the abrupt climate changes previously reported. Limited predictability is possible.

© 2011 Elsevier B.V. All rights reserved.

1. Introduction

Centuries ago South American sailors observed that during some years large increases in coastal tropical Pacific Ocean temperatures occurred in late December [1,2]. The scientific conclusion from these observations is that when El Niño Southern Oscillation (ENSO) effects occur that they are phase locked to the annual climate cycle. Perhaps the first scientific report of phase locking between ENSO and the annual cycle was by Bjerknes in 1969 [3]. He studied the Sea Surface Temperature (SST) and the wind velocities at Canton Island (Equatorial mid-Pacific) for the period 1962–1967 and reported:

"... sequence of rhythmic changes of temperature of approximately 2-year periodicity. ... The main maxima of SST in late 1963 and late 1965 coincide with the main minima of the [annual] easterly wind component."

showing phase locking at subharmonics of the annual frequency. Rasmussen and Carpenter [4] in 1982 showed that the maximum SST anomalies in the central tropical Pacific near 170W occurred at the end of the calendar year – again indicating phase locking to the annual cycle. Later, Rasmussen, Wang and Ropelewski [5] in 1990 identified a biennial mode in SST data that was phase locked with the annual cycle. They describe the period 1960–1970 as a well organized biennial regime. Wang and Wang [6] in 2000 studied the monthly tropical Pacific SST anomalies and found phase locking of the SST signal to subharmonics of the annual cycle. They stated that

"The biennial cycle (2–3 yr) appears to be significant in mid-1960s."

which is what had been reported by Bjerknes as 2 years.

Gu and Philander [7] in 1995 identified the annual cycle with the Sun: *"... The seasonal cycle, the forced response of the earth's climate to the periodic change in the solar radiation...."*

The objective of this Letter is to characterize the properties of the El Niño/La Niña phenomenon from the observational data without reference to any model. However, many models of the El Niño/La Niña phenomenon have a climate forcing at 1 cycle/year which causes a response at subharmonics of 1 cycle/year. These will be discussed briefly in Section 5.

The outline of this Letter is as follows. Section 2 gives the sources of the data. Various indices are defined and classification of the possible phase-locked states is given in Section 3. The observed phase-locked states are described in Section 4. Section 5 contains the discussion and Section 6 is the summary.

2. Data

All data are monthly time series.

2.1. Sea Surface Temperature (SST)

Barnston, Chelliah and Goldenberg [8] (BCG) in a general study with the objective of finding the location in the tropical Pacific with the strongest correlation with the core ENSO phenomenon determined that sea surface Region 3.4 (latitude: 5S to 5N; longitude: 120W–170W) that overlaps previously defined Region 3 and Region 4 was best. The average SST of Region 3.4 is named *SST3.4* and ranges between 24°C and 30°C. BCG defined a corresponding index of anomalies, *Nino3.4*, which is *SST3.4* with the

Table 1

Nine volcanoes since 1860 (all dates have an uncertainty of ±4 months).

| Volcanoes (maximum AOD greater than 0.04) | | | | Possible association with begin/end of a phase-locked segments (this study) | |
| Observations | | AOD (Sato et al. [13]) | | | |
Name of volcano	Date of beginning	Date of max	Value at max	Segment date	Segment #
Krakatau, Indonesia	Aug 1883	Apr 1884	0.132	Jun 1885	begin seg 1
Tarawera, New Zealand	Jun 1886	Oct 1886	0.069	none	none
Mont Pelée, Martinique and Soufrière	Mar 1903	Mar 1902	0.082	none	none
Katmai, Alaska	Jun 1912	Aug 1912	0.040	Jan 1912	begin seg 3
Argung, Bali	Feb 1963	Aug 1963	0.088	Feb 1963	begin seg 5
Fernandina, Galapagos	Jun 1968	Nov 1968	0.047	Aug 1969	begin seg 6
Fuego, Guatemala	Oct 1974	May 1975	0.040	Nov 74/Jan 75	end seg 6/begin seg 7
El Chichón, Mexico	Mar 1982	Dec 1982	0.098	Jan 1984	end seg 7
Pinatubo, Philippines	Jun 1991	Feb 1992	0.149	Dec 1991	begin seg 9

Seven of nine volcanoes may be associated with a phase-locked state.

seasonal effect "removed" by the climatology method that "... *may be regarded as an appropriate general SST index of the ENSO state by researchers, diagnosticians, and forecasters.*"

The Climate Prediction Center (CPC) of NOAA posts monthly values of *SST3.4* and *Nino3.4* which begins in 1950 [9]. Values of *SST3.4* beginning in 1856 used in this study were calculated from the longitude/latitude SST grid values from the Extended Reconstructed Sea Surface Temperature version 3b (ERSST3b) [10]. For a description of this data set see Smith, Reynolds, Peterson and Lawrimore [11]. The average SST, the low frequency index N_L and the high frequency index N_H (both defined below) were computed. The CPC also posts the value of the *Nino3.4* index from ERSST3b since 1950. Comparison of ERSST3b N_L values calculated here were compared to N_L values calculated from the *Nino3.4* values given by CPC. The correlation was greater than 0.99.

2.2. Aerosol Optical Density (AOD)

Some explosive volcanoes emit SO_2 that later becomes aerosols that reflect radiation from the Sun causing global cooling. The aerosol optical index (AOD) is the commonly used proxy for volcano climate forcing. The magnitude of AOD reaches a maximum several months after the eruption and decays thereafter. The delayed response of the climate system to the volcanic aerosols is 4 to 6 months [12]. The AOD data and list of volcanoes used in this Letter are from Sato, Hansen, McCormick and Pollack [13]. Nine volcanoes had a maximum in AOD larger than 0.04 since 1880 and are listed in Table 1.

3. Methods and definitions

3.1. The 12-month digital filter $\mathcal{F}$

Consider monthly time-series data that have been put through the digital filter

$$\mathcal{F} = \text{12-month symmetric moving average "box"} \\ \text{digital filter.} \tag{1}$$

This filter is a low pass filter that allows frequencies lower than $(1/12)$ month^{-1} to pass with only slight attenuation. This filter has an additional important property that is not generally recognized. The Fourier transform of $\mathcal{F}_{12}$ is $H_{12}(f) = \sin(\pi 12 f)/\sin(\pi f)$, which has zeros at multiples of the frequency $f = (1/12)$ month^{-1} [14]. Thus, signals whose frequencies are exactly $f = (1/12)$ month^{-1} and its harmonics are removed. This second property is highly desirable in reducing an unwanted seasonal signal that contains an annual component and its harmonics. One frequently sees the use of k-month filters where k has values 3, 5, 7, 9, 11, 12, 13 in attempts to reduce the seasonal signal; the

$k = 12$ filter is obviously best for removal of such a signal. Because the center of the filter is between time series data points, one has to place the center of the filter one half interval before or after the reference data point. Here, the choice is "after". The 12-month filter is then described as "6-1-5", where "1" is the reference. There is a loss of six data points at the beginning of the time series and five at end of the time-series.

3.2. Climate indices

Douglass [15,16] found that the widely used El Niño/La Niña anomaly index *Nino3.4*, created by subtracting from the *SST3.4* data the climatology (constant seasonal values), contains a substantial component of the seasonal effect. In addition, it was shown that no set of climatology values would remove the seasonal signal. A different scheme that does not use the climatology method was given using filter $\mathcal{F}$. The new "season free" El Niño/La Niña index is defined by

$$N_L(SST3.4) = \mathcal{F}(SST3.4) - \text{average } \mathcal{F}(SST3.4), \tag{2}$$

where the average is over the 30-year baseline, 1981–2010. (The subscript L stands for low pass.) A second index from *SST3.4* was also defined:

$$N_H(SST3.4) = SST3.4 - \mathcal{F}(SST3.4), \tag{3}$$

which contains the seasonal effect. This index shows a strong periodicity of 1 year. (H stands for high-pass.) As pointed out in Douglass [16], N_L and N_H are mathematical operations that can be applied to any geophysical time series. Since this study only considers the *SST3.4* time series, the symbols N_L and N_H will represent $N_L(SST3.4)$ and $N_H(SST3.4)$ respectively.

3.3. Definitions related to phase locking to the annual cycle

As will be shown below both N_L and N_H are phase locked to the annual cycle. Definitions associated with relative phase locking are now given.

Parity. The average monthly values of N_H show a maximum during Apr/May/June (AMJ). See Fig. 1(e). The maximum of the average monthly magnitude of N_L occurs during Nov/Dec/Jan (NDJ). Thus, an N_L phase-locked time segment is found in one of two parity states relative to N_H:

Ortho parity: if the maxima of N_L occur during NDJ. (4a)

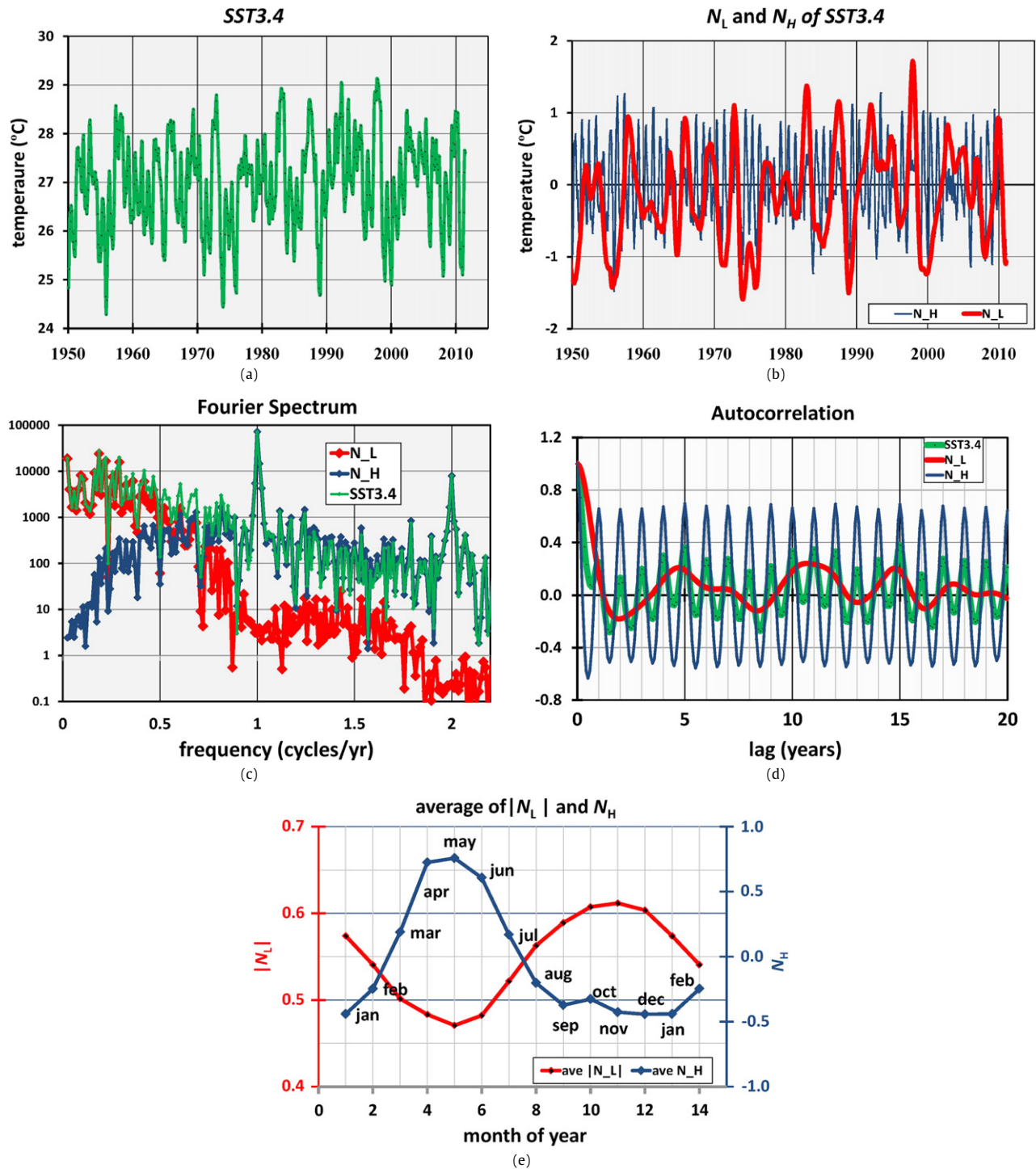Para parity: if the maxima of N_L occur during AMJ. (4b)

Fig. 1. Plots associated with *SST3.4*: (a) Sea surface data *SST3.4* (in °C) (green). (b) El Niño/La Niña index N_L (red) and high frequency index N_H (blue) (in °C). (c) Fourier spectrum of *SST3.4* (green), N_L (red) and N_H (blue). (d) Autocorrelation of *SST3.4* (green), N_L (red) and N_H (blue). (e). Average monthly values of $|N_L|$ (red) and N_H (blue). (For interpretation of the references to color in this figure legend, the reader is referred to the web version of this Letter.)

Subharmonic number n. This is the number of annual oscillations during one oscillation of N_L.

Equivalent substates. If N_L is phase locked to the nth subharmonic of the annual frequency, then there are n annual oscillations to one of N_L and thus there are n equivalent maxima. The n equivalent substates are indexed by *mod index* = annual (mod N_L), where the mod index has the values $[0, 1, \ldots, n-1]$. For example, a segment with period 3 years has three equivalent mod states that can be indexed by 0, 1, and 2.

Thus, the characterization of a phase-locked state requires three discrete indices: parity, subharmonic number and mod index. Table 2 lists the various defined quantities.

3.4. Determination of periodicity in a subharmonic N_L time segment

Two complimentary ways were used to determine the period.

(1) Inspection. In the record since 1856 most maxima in N_L occurred during NDJ; i.e., the intervals are multiples of 12 months.

Table 2
Definitions of various quantities.

Definitions of various quantities		
Region 3.4	Area in central Equatorial Pacific: [5S to 5N; 120W to 170W]	A primary reference area for ENSO phenomena
SST3.4	Monthly values of the average Sea Surface Temperature (SST) over Region 3.4	Ranges between 24 °C and 30 °C. Consists of ENSO effect plus a seasonal effect.
Climatology	For monthly data the Climatology is a set of 12 constant numbers that are an average of *SST3.4* for each month over a fixed period (usually 30 years).	Used in the construction of index *Nino3.4*.
Nino3.4	The commonly used index of anomalies defined as *SST3.4* minus the climatology	Shows the familiar El Niño/La Niña phenomena It is contaminated with the seasonal effect [15,16].
Filter $\mathcal{F}$	12-point symmetric moving average "box" digital filter	Separates the annual component and harmonics from a monthly time-series.
N_L	$N_L = \mathcal{F}(SST3.4) -$ average $\mathcal{F}(SST3.4)$	Introduced by Douglass [15] as an alternate to *Nino3.4*. This differs from *Nino3.4* because *Nino3.4* still contains some of the seasonal signal.
N_H	$N_H = SST3.4 - \mathcal{F}(SST3.4)$	A new index that is predominately a signal at a frequency of 1/year. This index contains the seasonal signal.
Three quantities to characterize phase-locked N_L segments of periodicity *n* years		
Parity: *P*	Para parity: if the maxima of N_L occurs during April/May/June Ortho parity: if the maxima of N_L occurs during Nov/Dec/Jan	
Subharmonic number: *n*	*n* is the number of annual oscillations during one oscillation of N_L.	
Equivalent substates: mod index	The *n* equivalent substates are indexed by mod index = *annual* (mod N_L), where the mod index can take on one the values $[0, 1, \ldots, n-1]$.	

Thus the search for segments of fixed periodicity can consist of looking at segments where successive maxima are the same multiple of 12 months apart. Many segments of period 24 months or 36 months are apparent. For example, the 1896–1908 segment clearly shows four cycles of period 36 months. See Fig. 2(a).

(2) Autocorrelation. The period of oscillation of a candidate time segment can be ascertained from the autocorrelation function vs. lag time τ of that segment. If there is an underlying periodicity then the autocorrelation function will have a maximum at a τ equal to the underlying period. These results should confirm any preliminary result from method (1). Equally important, this test allows the beginning and end dates of a segment to be determined with a relative accuracy of several months by finding that beginning or end date when the period starts to change. Adjacent phase-locked time segments with the same period but different parity or mod index are easily distinguished.

4. Analysis of data

4.1. SST indices, Fourier spectrum and autocorrelation

Fig. 1(a) shows the monthly values of the *SST3.4* time series (only from 1950 to 2010). One sees an oscillatory signal that ranges in amplitude from 24 to 30 °C. Fig. 1(b) shows N_L (in red) and N_H (in black). Fig. 1(c) shows the Fourier spectrum of *SST3.4* (green), N_H (blue) and N_L (red). In the discussion of this plot, low frequency means less than 1 cycle/year and high frequency means 1 cycle/year and higher. The spectrum of *SST3.4* is seen to have a broad peak at low frequencies and at high frequencies a large peak at 1 cycle/yr with a smaller peak at the 2nd harmonic. As expected, application of filter $\mathcal{F}$ to produce N_L and N_H shows that: (1) the spectrum of N_L has had the high frequencies greatly attenuated which includes both the peak at 1 cycle/year and its 2nd harmonic; (2) the spectrum of N_H has had the low frequencies greatly attenuated and that the main features are the maximum at

1-cycle/year and the maximum at the 2nd harmonic whose magnitude is about 10 times smaller.

Fig. 1(d) shows autocorrelation vs. delay τ. The N_H plot shows an abrupt drop in amplitude at zero delay from 1.0 of about 0.4, which is the "stochastic" component. For delays greater than 1 year, the autocorrelation function becomes a signal of period 1 year and amplitude of 0.6. The negative values of the periodic signal are "flat" because of the presence of a 2nd harmonic. The maxima of the periodic signal occur exactly at yearly integer values of τ to at least 100 years (not shown). These later oscillations are exactly in phase with earlier values. This coherence at long lag times implies a sustained oscillation. Also, the phase accuracy rules out the remote possibility that the period is one sidereal year rather than one solar year.

The average over the record of N_H for each month of the year was also computed. The plot of the 12 values in Fig. 1(e) shows a maximum during April/May/June and a flat minimum during Nov/Dec/Jan. Also shown in Fig. 1(e) is the average of the magnitude of N_L for each month, where is seen that the maximum occurs during Oct/Nov/Dec. Index N_L does not show annual oscillations (next section); however, when maxima in N_L do occur they will coincide with either a maximum or minima in N_H. These are the two parity states described above.

4.2. Phase-locked states of N_L of period 2 or 3 years

Figs. 2(a)–(e) show that there are at least ten phase-locked time segments of N_L where the period of the phase-locked state is exactly two years or three years. For these cases, the parity of the state is determined by the tests in Section 3.3. The period is verified by the tests in Section 3.4. The relative mod index is determined by setting the value for the most recent time segment of its kind equal to 0. For example, the mod index of segment #9 in Table 3 (July 1991 to June 2001; period three years, parity = ortho) was set to 0 which determined that the mod indices for segments #1, #2, #3, #6 and #7 were 2, 1, 1, 2 and 0 respectively.
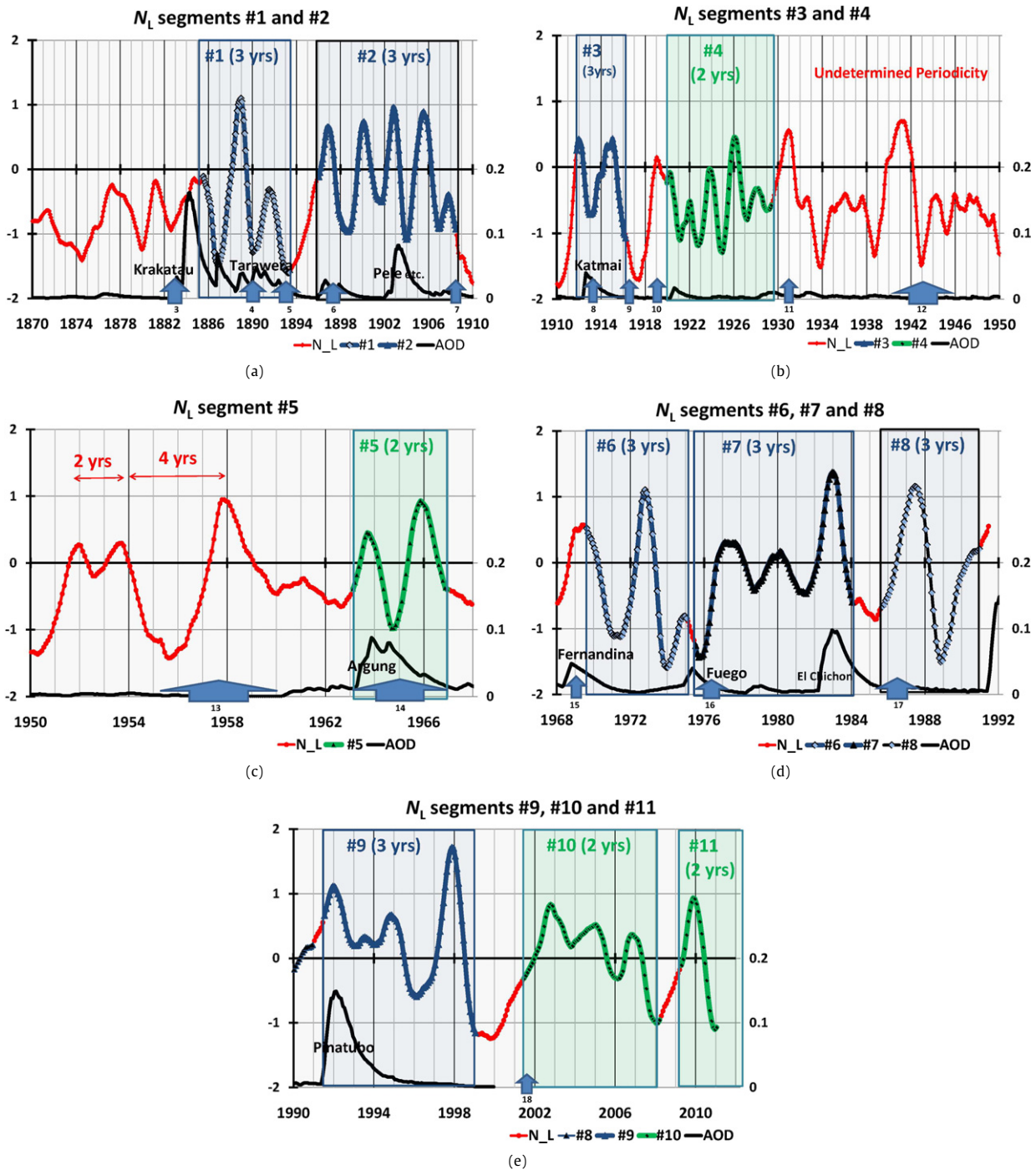
Fig. 2. El Niño/La Niña index N_L and volcano proxy AOD (black). Ten distinct phase locked time segments are indicated. Segments 1, 2, 3, 6, 7, 8 and 9 have period 3 years (blue shaded boxes). Segments 4, 5, 10 and 11 have period 2 years (green shaded boxes). Segment 8 is the only segment to have "para" parity. The dates of the eighteen abrupt climate shifts reported by Douglass [18] are indicated by numbered arrows. The width of the arrow shows the date range. The volcano AOD index (scale to right) is plotted in black. (a) 1870 to 1910, (b) 1910 to 1930, (c) 1950 to 1968, (d) 1968 to 1992, (e) 1990 to 2012. (For interpretation of the references to color in this figure legend, the reader is referred to the web version of this or Letter.)

Segment 1. (June 1885 to April 1893). This time segment shows two cycles of period 3 years. The parity is ortho and the mod index is 2.

Segment 2. (Jan 1896 to June 1908). This time segment shows four cycles of period 3 years (noted in Douglass [15]). The parity is ortho and the mod index is 1. After the end of this time segment it appears that one cycle of period 2 years occurs followed by 4 years of undefined period.

Segment 3. (Jan 1912 to Jan 1917). This segment shows nearly two cycles of period 3 years. The parity is ortho and the mod index is 1.

Segment 4. (Dec 1919 to Jan 1929). This segment shows five cycles of period 2 years. The parity is ortho and the mod index is 1.

[From 1930 to 1960 no time segment could be identified according to the criteria of Section 3.3. However, from 1952 to 1958

Table 3
Ten phase-locked time segments in N_L of period 2 or 3 years.

N_L(SST3.4) phase-locked segments of 2- and 3-year period					Climate shifts (Douglass [18])		
Seg #	Date (±4 months) (N_L)	Parity	Mod index		Minimum in diameter D		
			2-year	3-year	Min #	Date	Comment
1	Jun 1885–Apr 1893 (−1.3)	ortho		2	3	1982–1984	Begin seg 1
					4	1889–1991	End of seg 1?
					5	1894–1995	End of seg 1?
2	Jan 1896–Jun 1908 (−0.6)	ortho		1	6	1897–1998	Begin seg 2
					7	1908–1909	End seg 2
3	Oct 1911–Feb 1916 (−0.8)	ortho		1	8	1912–1913	Begin seg 3
					9	1916–1917	End seg 3
4	Dec 1919–Jun 1929 (−0.2)	ortho	1		10	1919	Begin seg 4
					11	1931	End seg 4
					12	1941–1945	?
					13	1956–1959	?
5	Feb 1963–Dec 1966 (−0.1)	ortho	1		14	1964–1966	Begin to end seg 5
6	Aug 1969–Jan 1975 (−0.6)	ortho		2	15	1969	Begin seg 6
					Weak min	1975	End seg 6
7	Jan 1975–Jun 1984 (−0.3)	ortho		0	16	1976–1977	Begin seg 7
					None		
8	Sept 1985–Dec 1990 (+0.4)	para		0	17	1986–1987	Begin seg 8
					Weak min	1990–1991	End seg 8
9	Jun 1991–Jan 1999 (−0.9)	ortho		0	Weak min	1992–1993	Begin seg 9
					18	2001–2002	End seg 9
10	Jun 2001–Mar 2008 (−0.8)	ortho	0		18	2001–2002	Begin seg 10
					No data		
11	Apr 2009–?	ortho	1		No data		

there appears to be one cycle of period 2 years followed be one cycle of period 4 years.]

Segment 5. (Feb 1963 to Dec 1966). This time segment, first identified by Bjerknes [4], shows two cycles of period 2 years. The parity is ortho and mod index = 1.

Segment 6. (Aug 1969 to Nov 1974). This segment shows nearly three cycles of period 3 years. The parity is ortho and the mod index is 0. The 1st maximum is the well known El Niño of 1973–1974.

Segment 7. (Jan 1975 to Jan 1984). This segment shows nearly three cycles of period 3 years. The parity is ortho and mod index is 0. The last maximum is the well known El Niño of 1983–1984.

Segment 8. (Sept 1985 to Dec 1990). This segment shows about 1.5 cycles of period 3 years. The parity is clearly "para" because N_L has its maximum during AMJ. This is the only time segment found to have this parity.

Segment 9. (Dec 1991 to Dec 1999). This time segment has period 3 years. The parity is ortho and the *mod* index is 0. The third maximum is the well known El Niño of 1997–1998.

Segment 10. (June 2001 to Mar 2008). This segment shows more than three oscillations of period 2 years. The parity class is ortho and the mod index is 0.

Segment 11. (This phase-locked state began about April 2009). This segment is not long enough (in Aug 2011) to determine its state although it appears to be period 2 years.

No period could be identified for the time intervals between these listed segments. This could be because the time segment is too short, or the climate system is "hunting" for a stable subharmonic state or that the system is chaotic.

5. Discussion

5.1. Subharmonic phase locking

The phenomenon of subharmonic phase-locking is well known in the field of nonlinear dynamics. Stoker [17] shows that for the example of a 1-D nonlinear oscillator of intrinsic frequency f_0 driven by a forcing F at frequency f_F, there is a direct response N_1 at f_F opposite in phase with that of F. In addition, there may at the same time be a phase-locked response at a subharmonic of f_F. In particular, a response of amplitude $N_{1/3}$ at the third subharmonic is possible. The conditions for $N_{1/3}$ to exist involve the nonlinear coefficient, the amplitudes and the difference between $f_F/3$ and f_0 as well as other quantities. If these conditions are not satisfied there are no solutions for $N_{1/3}$. A solution, if generated, will terminate abruptly if variation of the amplitudes or nonlinear parameter causes the conditions not to be satisfied.

The phase-locking phenomena reported in this Letter are very similar to the results for the 1-D nonlinear oscillator. An annual solar forcing F_S postulated in Section 5.4 below causes a response N_H at the annual frequency. Simultaneously, a subharmonic phase-locked response signal N_L may exist that may also abruptly begin and end. The comparisons are summarized in Table 4.

5.2. Correspondence with known climate shifts

Douglass [18] reported in a study of a set of global climate indices that the topological diameter D measures phase locking and that the minima in D are identified with climate shifts. Eighteen

Table 4

Comparison of properties of Pacific region *SST3.4* and the 1-D nonlinear oscillator.

	1-D nonlinear driven oscillator (Stoker [18])	Study of *SST3.4* indices N_H and N_L
External forcing	$F = F_0 \cos 2\pi f_F t$ at frequency f_F	Inferred solar F_S at frequency 1 year^{-1}
Direct response	$N_L \propto -F$ at frequency f_F	$N_H \propto -F_S$ at frequency 1 year^{-1}
Subharmonic response	$N_{1/n} \propto -N_1$ at subharmonic of f_F ($n = 3$, for example). Permitted if conditions involving amplitudes and nonlinear coupling constants are satisfied – otherwise no solution.	$N_L \propto -N_H$ at subharmonic of 1 year^{-1} (sometimes observed)

strong events since 1880 were identified. There is a near one-to-one correspondence between the 20 beginning/end dates of the 10 coherent states found in this Letter and the list of climate shifts in [18]. See Table 3. For example, the 3-year period segment (#2) from 1895 to 1908 in this study corresponds to climate shifts #2 and #3. A second example is segment #4 from 1919 to 1929 that consists of five cycles of period 2 years corresponding to climate shifts #6 and # 7. More recently a phase-locked segment of period 2 years from 2001 to 2008 corresponds to shifts #18 and #19.

5.3. What causes the abrupt changes in phase locking?

This study shows that the phase-locked subharmonic states may end/begin abruptly. Abrupt changes suggest impulses to the climate system.

5.3.1. El Niños?
El Niños can be ruled out because the most recent large El Niños (1973–1974, 1983–1984 and 1997–1998) do not correspond to any of these abrupt shifts.

5.3.2. Volcanoes?
The magnitude of the volcano AOD proxy reaches a maximum several months after the eruption and the response of the climate system is delayed 5 to 6 months [19]. Even though the climate effect is transitory the coupling during the impulse might be sufficiently strong to cause a transition from/to a different phase-locked state. The AOD data [13] plotted in Fig. 2 shows nine volcanoes since 1870 whose maximum in AOD is greater than 0.04. See Table 1. The occurrence of seven of the nine volcanoes are sufficiently close to the beginning/end dates of one of the phase-locked segment to suggest an association (Krakatau, Katmai, Argung, Fernandina, Fuego, El Chichón and Pinatubo). The remaining two volcano events (Tawawera and Pelée) occurred during the middle of a phase-locked segment. The dates of the Fuego, Argung and Pinatubo volcanoes are particularly close to the beginning of a phase-locked segment.

The eruption of Fuego occurred on Nov 1974 and the AOD index reached a maximum on Mar 1975 near the dates of the abrupt change between phase-locked segments 6 and 7. These two 3-year period phase-locked segments differ only in their mod index. There is a very interesting and well documented climate event that may be associated with this abrupt change in the phase-locked state and the Fuego eruption. This is the "aborted event of 1975" described by Busalacchi, Takeuchi, and O'Brien [20]. Prior to the aborted event, Wyrtki and Quinn had both stated in 1974 "... [that] *another El Niño might be expected at the beginning of 1975*." (Wyrtki et al. [21]). Two cruise expeditions to the Equatorial eastern Pacific were quickly organized for the University of Hawaii's research vessel. *R.V. Moana Wave.* Cruise 1 was from Feb 11 to Mar 31, 1975. Cruise 2 was from April 17 to May 25, 1975. Wyrtki et al. summarized: "... [the] *first cruise ... showed all the features of a starting El Niño, ... the second cruise showed that it was short lived*."

These observations can possibly be explained by the results of this Letter. Prior to Jan 1975 the climate system was in a 3-year, mod index 2, ortho state. Between the 1st and 2nd cruises an abrupt climate change (Fuego?) happened that caused the climate system to change from mod index 2 to mod index 0. [The slight mismatch of dates may be explained by the fact that the expeditions were in the eastern Pacific while the N_L index derives from the central Pacific.] Changing from mod 2 to 0 is equivalent to "jumping back" two years – i.e. the time series for N_L after 1975 appears to join smoothly if translated back in time by two years.

There are not enough large volcanoes to explain all of the observed abrupt climate changes. An additional possibility is considered in the next section.

5.3.3. Stability limits of the phase-locked state?
In the forced 1-D nonlinear example discussed in Section 5.2 there is a response at the forcing frequency f_F. There may at the same time be a phase-locked response at a particular subharmonic of f_F if certain conditions involving the nonlinear coupling and the amplitudes are met. If these conditions vary (such as a change of amplitude), then the subharmonic solution could be unstable and an abrupt change to a new state must occur. This possibility will be the subject of a later paper.

It is noted that for 9 of the 10 completed time segments that termination occurs at a negative value of N_L (listed in Table 3). Segment #8 appears to be an exception but this segment has the opposite parity so one might expect the sign of the N_L termination to be opposite also.

5.4. Climate forcing of N_H (and N_L)

What causes N_H? The autocorrelation of N_H shows sustained oscillations at a frequency of 1 (solar year)$^{-1}$. That the oscillations are sustained implies that there is an external forcing. From the fact that the frequency is 1 (solar year)$^{-1}$ further implies that the external forcing is of solar origin. Let F_S be a proxy forcing for all the annual climate processes [direct and indirect] associated with the Sun. Using this terminology, the annual oscillations of F_S causes the annual oscillations in N_H, which would be of opposite phase. Index N_L is also phase locked to the solar annual cycle. Thus, the solar climate forcing F_S causes both N_L and N_H. A corollary of this statement is that N_H does not cause N_L.

The existence of phase-locked segments in N_L is not in conflict with the nearly Gaussian distribution of N_L values found by Douglass [15] because the distribution can be caused in part by the "random" occurrence of the beginning and ends of these segments.

5.5. Comparison to models

There are a number of papers in which models are proposed whose solutions have many of the features found in this study. Cane and Ziebiak [22] (CZ) proposed a coupled tropical ocean-atmosphere model of El Niño and Southern Oscillation that has

been used by later investigators. Battisti [23] and also Barnett et al. [24] have explicitly considered seasonal (period 1 year) forcing within the CZ model. In 1994–1995 three papers were published nearly simultaneously: Jin et al. [25]; Tziperman et al. [26] and Chang et al. [27]. All showed that subharmonics of the seasonal forcing may occur under some conditions. In a later paper, Jin et al. [28] showed that seasonal forcing produced both a response at the seasonal cycle and the ENSO mode. In addition, Jin et al. showed that the amplitude of the seasonal response and the ENSO signal are out of phase with each other.

A paper is being written with a discussion of these models and the results of this study.

5.6. Predictability

Predicting future El Niño/La Niño phenomenon depends upon knowledge of the past and an extrapolation to the future that assumes continuity of the relevant climate variables. Unfortunately, the assumption of continuity across an abrupt climate shift is not warranted. However, limited predictability is possible if the climate system is known or likely to be in a phase-locked subharmonic state. While in this state the period is known and the dates of future possible maxima [El Niños] and minima [La Niñas] are determined. For example, the El Niño of 1997–1998 is one of the maxima in a time-segment of period 3 years that began in late 1991. The period of this segment could have been determined by 1995 and also the future date of the 1997–1998 El Niño. Equally important, while in this state the dates when an El Niño will *not* occur are also determined.

At about April 2009 a new climate state began tin which N_L showed a maximum in Nov/Dec 2009 and a minimum in Nov/Dec 2010. This state may be of period 2 years. If so, the next maximum will be in Nov/Dec 2011.

6. Summary

It is shown that the central Pacific sea surface data consists of two components: N_L, a low frequency signal that exhibits the familiar El Niño/La Niña phenomenon and N_H, a high frequency signal of one-year period. A surprisingly simple explanation of some of the observed phenomenon comes from an analysis of these signals. In this scenario, a forcing F_S of solar origin at a frequency of 1 year^{-1} exists, which can produce two phase-locked responses: a direct response N_H at a frequency of 1 cycle/year and also, because of nonlinear effects, can produce a response N_L which may be phase-locked to the 2nd or 3rd subharmonic of F_S. At least ten of these subharmonic time segments since 1870 have been identified. The beginnings or ends of these time segments have a

near one-to-one correspondence with the eighteen abrupt climate changes previously reported by Douglass [18].

The well known El Niños of 1973–1974, 1983–1984 and 1997–1998 are simply a positive cycle of one of the oscillations in particular 3-year period phase-locked segments. If the climate system is known to be in one of these phase-locked states, limited predictability is possible.

Acknowledgements

References

[1] S.G. Philander, El Niño, La Niña and the Southern Oscillation, Academic Press, 1990.
[2] M.H. Glantz, Currents of Change, Cambridge University Press, Cambridge, UK, 2001.
[3] J. Bjerknes, Analysis of the rhythmic variations of the Hadley Circulation over the Pacific during 1963–67, Technical Report, ONR contract No. N0014-69-A-0200-4044 NR 083-287, 1969.
[4] E.M. Rasmusson, T. Carpenter, Monthly Weather Rev. 110 (1982) 354.
[5] E.M. Rasmusson, X. Wang, C. Ropelewski, J. Marine Syst. 1 (1990) 71.
[6] R. Wang, B. Wang, J. Atmos. Sci. 57 (2000) 3315.
[7] D. Gu, S.G.H. Philander, J. Climate 8 (1995) 864.
[8] A.C. Barnston, M. Chelliah, S.B. Goldenberg, Atmosphere–Ocean 35 (3) (1997) 367.
[9] ERSST3b, 2010, data at http://iridl.ldeo.columbia.edu/SOURCES/.NOAA/.NCDC/.ERSST/.version3b/.
[10] NOAA/CPC, 2009, SST data and indices are found at http://www.cpc.ncep.noaa.gov/data/indices/.
[11] T.M. Smith, R.W. Reynolds, T.C. Peterson, J. Lawrimore, J. Climate 21 (2008) 2283.
[12] D.H. Douglass, R.S. Knox, Phys. Lett. A 373 (2009) 3296, doi:10.1016/j.physleta.2009.07.023.
[13] M.J. Sato, J. Hansen, P. McCormick, J. Polak, J. Geophys. Res. 98 (1993) 22987, AOD data at http://data.giss.nasa.gov/modelforce/strataer/.
[14] S.W. Smith, The Scientists and Engineer's Guide to Signal Processing, California Technical Publishing, San Diego, CA, 1997, Chap. 15.
[15] D.H. Douglass, J. Geophys. Res. 115 (2010) D15111, doi:10.1029/2009JD013508.
[16] D.H. Douglass, Int. J. Geophys. 2 (4) (2011), in press.
[17] J.J. Stoker, Nonlinear Vibrations, Interscience Publishers, 1950.
[18] D.H. Douglass, Phys. Lett. A 374 (2010) 4164, doi:10.1016/j.physleta.2010.08.025.
[19] D.H. Douglass, R.S. Knox, B.D. Pearson, A. Clark, Geophys. Res. Lett. 33 (2006) L19711, doi:10.1029/2006GL026355.
[20] A.J. Busalacchi, K. Takeuchi, J.J. O'Brien, J. Geophys. Res. 88 (1983) 7551.
[21] K. Wyrtki, E. Stroup, W. Patzert, R. Williams, W. Quinn, Science 191 (1976) 341.
[22] M.A. Cane, S.E. Ziebach, Science 228 (1985) 1084.
[23] D.S. Battista, Sciences 45 (1988) 2889.
[24] T.P. Barnett, M. Latif, N. Graham, S. Pazan, W. White, J. Climate 6 (1993) 1445.
[25] F.F. Jin, J.D. Neelin, M. Ghil, Science 264 (1994) 70.
[26] E. Tziperman, L. Stone, M.A. Cane, H. Jarosh, Science 264 (1994) 72.
[27] P. Chang, L. Ji, B. Wang, T. Li, J. Atmos. Sci. 52 (1995) 2353.
[28] F.F. Jin, J.D. Neelin, M. Ghil, Physica D 98 (1996) 442.